REPORT DOCUMENTATION PAGE

Form Approved OMB NO. 0704-0188

The public reporting burden for this collection of information is estimated to average 1 hour per response, including the time for reviewing instructions, searching existing data sources, gathering and maintaining the data needed, and completing and reviewing the collection of information. Send comments regarding this burden estimate or any other aspect of this collection of information, including suggestions for reducing this burden, to Washington Headquarters Services, Directorate for Information Operations and Reports, 1215 Jefferson Davis Highway, Suite 1204, Arlington VA, 22202-4302. Respondents should be aware that notwithstanding any other provision of law, no person shall be subject to any penalty for failing to comply with a collection of information if it does not display a currently valid OMB control number.
PLEASE DO NOT RETURN YOUR FORM TO THE ABOVE ADDRESS.

1. REPORT DATE (DD-MM-YYYY)	2. REPORT TYPE	3. DATES COVERED (From - To)
19-01-2012	Final Report	18-Nov-2004 - 17-May-2011

4. TITLE AND SUBTITLE
Development of Flexible Extremities Protection utilizing Shear Thickening Fluid/Fabric Composites

5a. CONTRACT NUMBER
W911NF-05-2-0006

5b. GRANT NUMBER

5c. PROGRAM ELEMENT NUMBER
611104

6. AUTHORS
Mahesh Hosur, Norman Wagner, C.T. Sun, Vijaya Rangari, Jack Gillespie, Shaik Jeelani, Hassan Mahfuz

5d. PROJECT NUMBER

5e. TASK NUMBER

5f. WORK UNIT NUMBER

7. PERFORMING ORGANIZATION NAMES AND ADDRESSES
Tuskegee University
Tuskegee University
204 Kresge Center
Tuskegee, AL 36088 -1923

8. PERFORMING ORGANIZATION REPORT NUMBER

9. SPONSORING/MONITORING AGENCY NAME(S) AND ADDRESS(ES)
U.S. Army Research Office
P.O. Box 12211
Research Triangle Park, NC 27709-2211

10. SPONSOR/MONITOR'S ACRONYM(S)
ARO

11. SPONSOR/MONITOR'S REPORT NUMBER(S)
47303-MS-BCE.42

12. DISTRIBUTION AVAILIBILITY STATEMENT
Approved for Public Release; Distribution Unlimited

13. SUPPLEMENTARY NOTES
The views, opinions and/or findings contained in this report are those of the author(s) and should not contrued as an official Department of the Army position, policy or decision, unless so designated by other documentation.

14. ABSTRACT
ABSTRACT

A systematic approach was undertaken to enhance spike resistance of flexible body armor. A traditional STF composite is consisted of fumed silica particles (about 7 nm in diameter but highly agglomerated due to van der Waals forces), PEG, and Kevlar. PEG is added to an aqueous suspension of silica and the solution is evaporated to

15. SUBJECT TERMS
STF, Flexible Armor, Kevlar, Spectra, Spike Test, Knife Test

16. SECURITY CLASSIFICATION OF:			17. LIMITATION OF ABSTRACT	15. NUMBER OF PAGES	19a. NAME OF RESPONSIBLE PERSON
a. REPORT	b. ABSTRACT	c. THIS PAGE			Shaik Jeelani
UU	UU	UU	UU		19b. TELEPHONE NUMBER 334-727-8970

Received	Paper
2012/01/19 1: 41	Mahesh Hosur, Jessie Mayo, Eric Wetzel, Shail Jeelani. Studies on the fabrication and stab resistance characterization of novel thermoplastic-Kevlar composites, Solid State Phenomena, (02 2006): 0. doi:
2012/01/19 1 40	Tarig Hassan, Vijaya Rangari, Shaik Jeelani. Sonochemical synthesis and rheological properties of shear thickening silica dispersion, Ultrasonics Sonochemistry, (02 2010): 0. doi:
2012/01/19 1 38	Tarig Hassan, Vijaya Rangari, Shaik Jeelani. Synthesis, Processing and characterization of shear thickening fluid (STF) impregnated fabric composites, Materials Science and Engineering A, (01 2010): 0. doi:
2012/01/19 1 37	Jessie Mayo, Eric Wetzel, Mahesh Hosur, Shaik Jeelani. Stab and puncture characterization of thermoplastic-impregnated aramid fabrics, International Journal of Impact Engineering, (04 2009): 0. doi:
2012/01/19 1 23	Amanda Lim, Sergey Lopatnikov, Norman Wagner and John Gillespie. Investigating the transient response of a shear thickeningfluid using the split Hopkinson pressure bar technique, Rheol Acta, (06 2010): 0. doi:
2012/01/19 1 22	Amanda Lim, Sergey Lopatnikov and John Gillespie. Development of the split-Hopkinson pressure bar technique for viscousfluid characterization, Polymer Testing, (08 2009): 0. doi:
2012/01/19 0 25	Amanda Lim, Sergey Lopatnikov, Norman Wagner and John Gillespie. Phenomenological modeling of the response of a dense colloidal suspensionunder dynamic squeezing flow, Journal of Non-Newtonian Fluid Mechanics, (04 2011): 0. doi:
2012/01/19 0 29	Zhaoxu Dong, and C.T. Sun. Testing and modeling of yarn pull-out in plain woven Kevlar fabrics, Composites Part A: Applied Science and Manufacturing, (04 2009): 0. doi:
2012/01/19 0 34	Dennis P. Kalman · Norman J. Wagner. Microstructure of shear-thickening concentratedsuspensions determined by flow-USANS, Rheol Acta, (03 2009): 0. doi:
2012/01/19 0 33	Dennis Kalman, Richard Merrill, Norman Wagner, Eric Wetzel. Effect of Particle Hardness on the PenetrationBehavior of Fabrics Intercalated with DryParticles and Concentrated Particle-FluidSuspensions, Applied Materials, (11 2009): 0. doi:
2012/01/19 0 36	Amanda Lim, Sergey Lopatnikov, Norman Wagner, John Gillespie. An experimental investigation into the kinetics of a concentrated hard-sphere colloidal suspension during Hopkinson bar evaluation at high stresses, Journal of Non-Newtonian Fluid Mechanics, (04 2010): 0. doi:
2012/01/19 0 28	ZHAOXU DONG, JAMES M. MANIMALA AND C. T. SUN. MECHANICAL BEHAVIOROF SILICA NANOPARTICLE-IMPREGNATEDKEVLAR FABRICS, Journal of Mechanics of Materials and Structures, (05 2010): 0. doi:
2012/01/19 0 14	Hassan Mahfuz, Floria Clements, Vijaya Rangari, Vinod Dhanak, and Graham Beamson. Enhanced stab resistance of armor composites with functionalized silica nanoparticles, Journal of Applied Physics, (03 2009): 0. doi:

TOTAL: 13

Number of Papers published in peer-reviewed journals:

(b) Papers published in non-peer-reviewed journals (N/A for none)

Received	Paper

TOTAL:

Received	Paper
2012/01/17 1: 31	Zhaoxu Dong and C.T. Sun. Testing and Modeling of Yarn Pullout of Plain Woven Kevlar fabric, CompTest 2008. 2008/10/20 00:00:00, . : ,
2012/01/17 1: 30	Zhaoxu Dong and C. T. Sun. Modeling Nano-Particle Colloid/Fabric Composites, American Society for Composites (ASC). 2006/09/17 00:00:00, . : ,
2012/01/17 1: 18	Hassan Mahfuz, Vincent Lambert, Patrick Bordner and Vijaya Rangari. Development of Stab Resistant Body Armor Using Silated SiO2 Nanoparticles Dispersed into Glutaraldehyde, NSTI Nanotech 2008. 2008/05/04 00:00:00, . : ,
2012/01/17 1: 17	Floria Clements, Hassan Mahfuz, Eric Wetzel and Justin Stewart. M50/V50/A50 Method for Characterizing Stab Resistant Materials for Body Armor Applications, 2007 Society of Experimental Mechanics (SEM) Conference. 2007/06/03 00:00:00, . : ,
2012/01/17 1: 16	Hassan Mahfuz, Floria Clements and Justin Stewart. Development of Stab Resistant Body Armor Using Fumed SiO2 Nanoparticles Dispersed into Polyethylene Glycol (PEG) through Sonic Cavitation, NSTI-Nanotech 2006. 2006/05/07 00:00:00, . : ,
2012/01/17 1: 15	Floria Clements and Hassan Mahfuz. ENHANCING THE STAB RESISTANCE OF FLEXIBLE BODY ARMOR USING FUNCTIONALIZED SIO2 NANOPARTICLES, 16th International Conference on Composite Materials (ICCM-16), Kyoto, Japan. 2007/07/08 00:00:00, . : ,
2012/01/13 1: 13	J. B. MAYO, JR., M. V. HOSUR, S. JEELANI, E. D. WETZEL. Cut Behavior of High Performance Fibers, The 1st joint American- Canadian International Conference on Composites September 17, 2009. 2009/09/17 01:00:00, . : ,
2012/01/13 1: 12	H. Rao, , M.V. Hosur, , J. Mayo, Jr., , S. Burton, , S. Jeelani. Stab Characterization of Hybrid Ballistic Fabrics, 2009 Annual Society for Experimental Mechanics Conference, Albuquerque, NM, June 1-4, 2009.. 2009/06/02 01:00:00, . : ,
2012/01/13 1: 11	Jessie B. Mayo, Jr., , Andre Lewis, , Mahesh V. Hosur, , Shaik Jeelani. Cut Studies of Brittle and Ductile Fibers, SAMPE 2009 Conference, Baltimore, MD, May 2009. 2009/05/20 01:00:00, . : ,
2012/01/13 1: 10	Harish M Rao, Jessie Mayo. Jr., Mahesh V. Hosur, Shaik Jeelani. STAB CHARACTERIZATION OF BALLISTIC FABRICS IMPREGNATED WITH SHEAR THICKENING FLUID, Fall Meeting of the Society for Advancement of Materials and Process Engineering (SAMPE), Sept. 9-11, 2008, Memphis, TN. 2008/09/10 01:00:00, . : ,
2012/01/13 1: 9	M. V. Hosur, J. B. Mayo Jr., E. Wetzel, S. Jeelani. Studies on the Fabrication and Stab Resistance Characterization of Novel Thermoplastic-Kevlar Composites, International Conference on Materials for Advanced Technologies – ICMAT-2007, July 1-6, 2007, Singapore.. 2007/06/03 01:00:00, . : ,
2012/01/13 1: 8	J. B. Mayo, Jr. , M. V. Hosur, E.Wetzel, S. Jeelani. RESISTANCE OF NOVEL THERMOPLASTIC-KEVLAR COMPOSITES TO SPIKE PENETRATION, 2nd International Conference on recent advanced in composite materials, Feb. 20-23, 2007, New-Delhi, India. 2007/02/21 01:00:00, . : ,
2012/01/13 1: 7	Jessie Mayo B. Jr., , Mahesh V. Hosur, , Shaik Jeelani. Dynamic and Quasi-Static Stab Resistance of Thermoplastic and Silica-Polyethylene Glycol Gel Infused Fabrics, 22nd Annual Technical Conference of the American Society for Composites, . 2007/09/17 01:00:00, . : ,

TOTAL: 13

Number of Peer-Reviewed Conference Proceeding publications (other than abstracts):

(d) Manuscripts

Received	Paper

TOTAL:

NAME	PERCENT_SUPPORTED	Discipline
Harish Rao	0.50	
Sreedhar Reddy Poluchalla	0.50	
Jessie B. Mayo Jr.	0.50	
Jessie B. Mayo Jr.	0.70	
Amanda Lim	0.70	
Dennis Kalman	0.75	
James Manimala	0.75	
Z. Dong	0.75	
Floria Clements	0.75	
Vincent Lambert	0.75	
Justin Stewart	0.25	
Abiola Gaines	1.00	
Tarig Hassan	1.00	
Andrew Lewis	1.00	
Ron Egress	0.25	
FTE Equivalent:	**10.15**	
Total Number:	**15**	

Names of Post Doctorates

NAME	PERCENT_SUPPORTED
Jessie B. Mayo Jr.	0.75
Sergey Lopatnikov	0.50
Y. Zhou	0.25
Joe Deitzel	0.10
Bazle Gama	0.10
FTE Equivalent:	**1.70**
Total Number:	**5**

Names of Faculty Supported

NAME	PERCENT_SUPPORTED	National Academy Member
Mahesh Hosur	0.10	
Shaik Jeelani	0.05	
Vijaya Rangari	0.10	
Hassan Mahfuz	0.10	
Jack Gillespie	0.05	
Norman Wagner	0.05	
C.T. Sun	0.10	
FTE Equivalent:	**0.55**	
Total Number:	**7**	

Names of Under Graduate students supported

NAME
Jessie B. Mayo Jr.
Amanda Lim
Dinnis Kalman
Zhaoxu Dong
Total Number: 4

Names of other research staff

NAME	PERCENT_SUPPORTED
Dorothy Bernett	0.10
FTE Equivalent:	**0.10**
Total Number:	1

Sub Contractors (DD882)

Inventions (DD882)

Scientific Progress

Cut Resistance of High Performance Fibers

Jessie B. Mayo, Jr.[1,2],Mahesh V. Hosur[1], Shaik Jeelani[1], and E. D. Wetzel[2*]

[1]Tuskgee Center for Advance Materials, Tuskegee University, Tuskegee, AL 36088

[2]U.S. Army Research Laboratory, Aberdeen Proving Ground, MD 21005

For submission to (suggestions)
Textile Research Journal
Composites Science and Technology
Journal of Engineering Materials
Journal of Materials Science

Draft version date:
30 Sept 2010 (JBM)

Abstract

I. Introduction

Fibers are classified as organic (aramids, extended chain polyethylenes, aromatic polyester fibers, aromatic heterocyclic polymer fibers, etc.) and inorganic (carbon, glass, metals, carbides, oxides, etc.) and are used in several applications. These applications include but are not limited to automotive, sports, composites technology, and flexible body armor. The flexible body armor industry has utilitzed many types of fabrics woven from high performance fibers that show good resistance against ballistic threats. Some examples of fabrics that show good ballistic resistance are Kevlar, Twaron, Technora, PBO and Spectra. The fibers that make up these fabrics are elastic and have high tensile moduli (Duan et al., 2006).

Well known is the fact that most body armor technologies have sufficient resistance against ballistic threats but have less resistance against cut and puncture threats. Puncture refers to intrusion of a material by a pointed object such as an ice-pick or awl. The pointed object has a tendency to "window" or displace the fibers and yarns of the woven material so that the object can easily enter through the fabric. Cut/shear occurs when an instrument with a continuous cutting edge transversely fractures the yarns/fiber bundles causing immediate severance. Mayo et al. (2009) examined the cut resistance of neat and thermoplastic impregnated Kevlar. Mayo et al. found that heat pressing thermoplastic films into hydrophobic Kevlar 706 dramatically increased cut and puncture resistance of the woven fabric. Decker et al. (2007) increased the puncture resistance of Kevlar and other woven fabrics by impregnating the fabric with shear-thickening fluid. Erlich et al. (2003) examined the resistance of Zylon to sharp fragments by means of quasi-static penetration push testing. Anctil et al. used a regime of P1 knives, S1 knives, engineered spikes, and flechettes as characterization tools to examine woven fabric resistance. These woven fabrics included Kevlar, Twaron, Spectra, Dyneema and Zylon.

When the concern is the cut resistance of yarns or fiber bundles, there are notable works. Shin and Shockey (2003) developed a test for measuring the cut resistance of Zylon yarns. Such

the crosshead fixture of a 20 N load cell of an Instron 5500 (Grove City, PA) materials testing system.

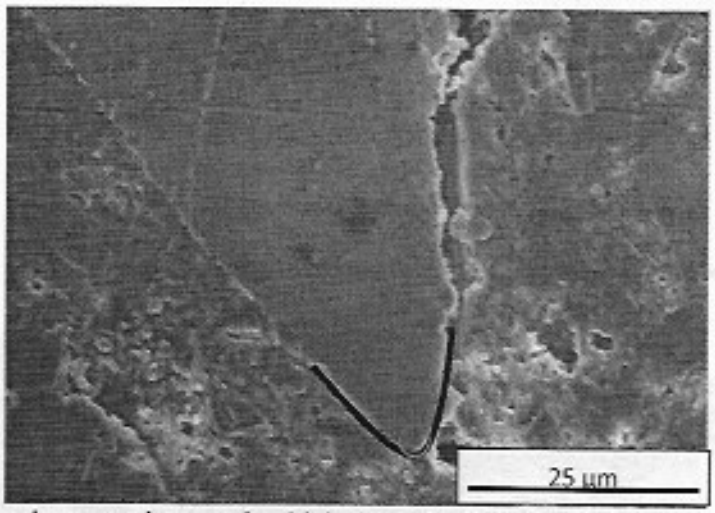
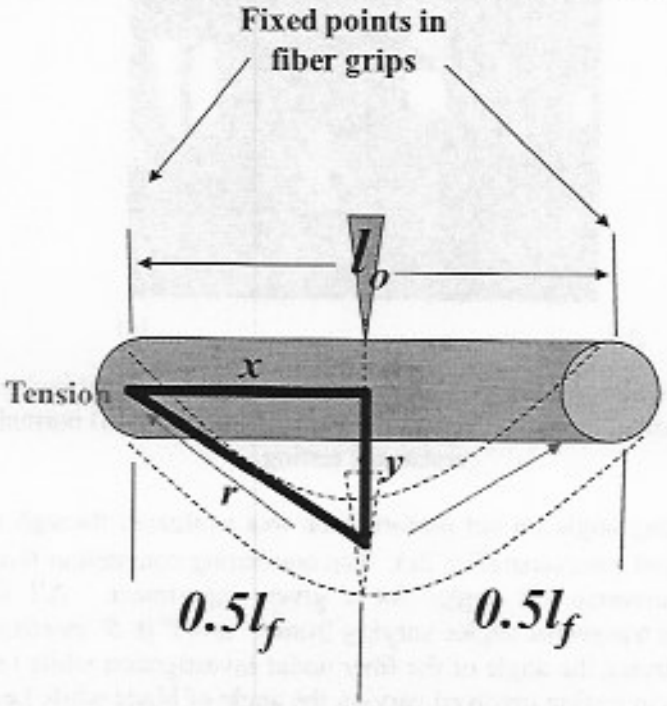


Figure 1. Scanning electron micrograph which show tip diameter (red circle) of Celanese blade.

The Celanese blade was used because of low error and data reproducibility. The blade has a tip radius of 14 µm. The blade cutting speed was maintained at 30 mm/min until the fiber was completely severed. Load vs. displacement curves were generated from the data obtained from the testing data.

The cut strain to failure was determined by using the Pythagorean theorem $x^2 + y^2 = r^2$.



III. Results

1. General behavior

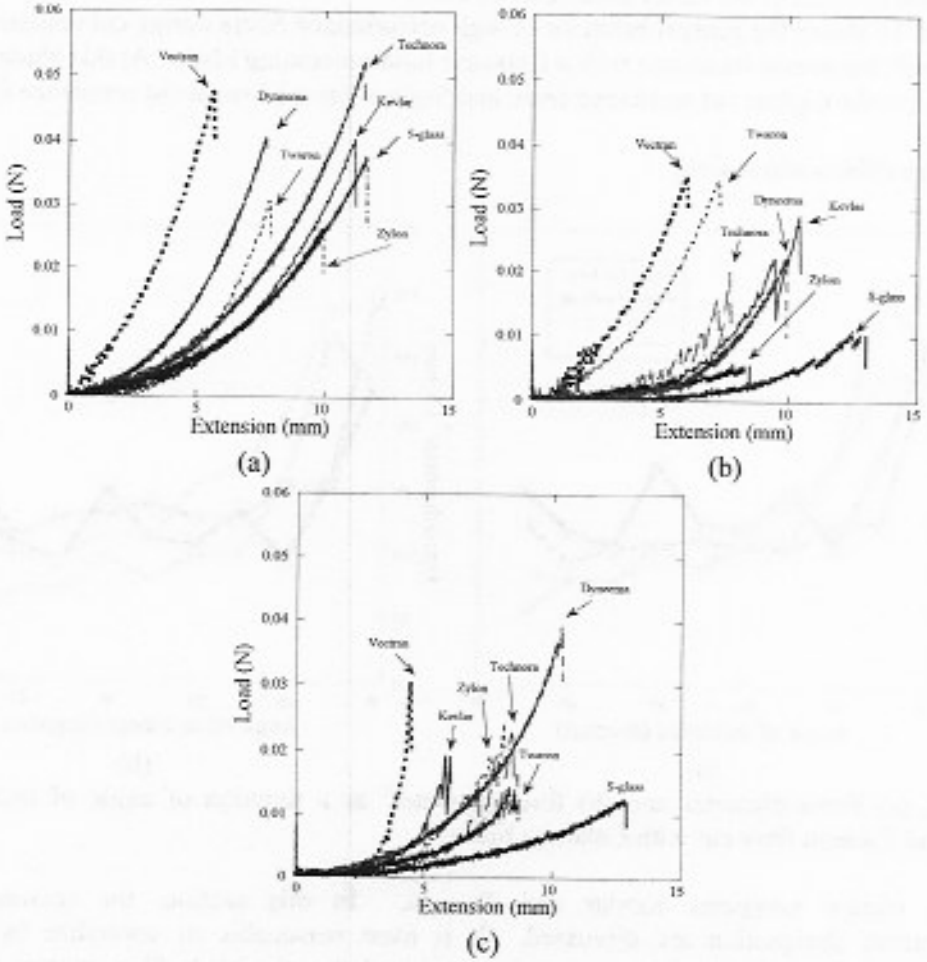


Figure 1. Force as a function of extension for high performance fibers cut at (a) normal incidence (0-0), (b) 45° longitudinal incidence (0-45) and, (c) 45° transverse incidence (45-0) by Celanese blade.

Figure 1a shows general behavior of high performance fibers during cut resistance testing at normal incidence with a Celanese food processing blade. This data is the raw data before diameter normalization. The raw data is given in Newtons (N) while extension is given in millimeters (mm). There is a gradual increase in load with extension/displacement for each fiber curve. The response drops to zero at failure. Without diameter normalization, Technora has highest cut resistance and Zylon has the lowest cut resistance.

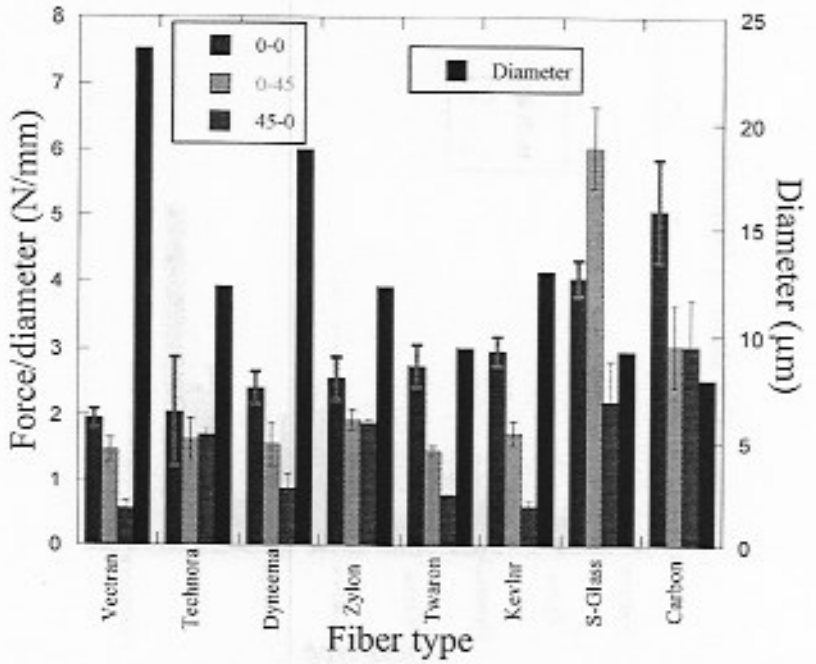


Figure 4. Force/diameter and diameter as a function of fiber type for all fibers tested for cut resistance at 0-0, 0-45, and 45-0.

Figure 4 is a plot of the force/diameter (left y-axis) and diameter (right y-axis) as a function of fiber type for all of the fibers that were tested for cut resistance. Fibers are listed with respect to magnitude of cut resistance at 0-0 from lowest to highest cut resistance. At 0-0 Vectran, the fiber with the largest diameter, has the lowest cut resistance. The reader must keep in mind that the diameter is a characterization tool because diameter effects have been discarded because of normalization. At 0-0 carbon fiber has the highest cut resistance. The two inorganic fibers are among the highest cut resistance cases. As the testing goes from 0-0 to 0-45 to 45-0, Vectran, Zylon, Twaron, Kevlar, and carbon fiber cut resistance decreases as the angle changes. S-glass is the only fiber where the 0-45 test is higher than 0-0 and 45-0.

Dyneema	2.42	2.04	1.98	1.43	1.46	1.61	1.00	1.20	1.43	1.56	1.61
Zylon	2.57	2.05	1.80	1.44	1.57	1.40	1.25	1.48	1.15	1.94	1.67
Vectran	1.96	1.80	1.87	1.32	1.75	2.02	1.56	1.66	1.75	1.47	1.72
Technora	6.67	1.61	1.27	1.31	1.31	1.38	1.58	1.79	1.23	1.63	1.98
S-glass	4.06	4.11	2.41	3.75	4.22	4.69	3.82	4.92	5.82	6.04	4.38
Carbon	5.08	5.26	5.68	7.29	5.88	5.76	4.34	4.52	5.61	3.05	5.25

Table 3. Summary of average force/diameter (N/mm) results of transverse cut resistance testing.

Fiber	0-0	0-5	0-10	15-0	20-0	25-0	30-0	35-0	40-0	45-0	Average
Kevlar	2.97	3.47	2.01	1.28	1.27	1.01	1.24	0.9	0.92	0.61	1.568
Twaron	2.76	2.13	1.53	1.24	1.14	0.82	0.85	0.7	0.71	0.77	1.265
Dyneema	2.27	0.96	1.14	1.73	0.73	1.04	0.6	0.81	0.64	1.8	1.172
Zylon	3.52	2.96	2.33	1.65	1.1	1.33	0.86	0.86	0.55	1.9	1.706
Vectran	1.96	2.93	1.52	1.52	1.38	1.18	0.63	0.94	0.65	0.56	1.331
Technora	4.13	2.73	2.22	1.74	1.23	1.37	1.25	0.79	0.9	1.7	1.806
S-glass	4.19	4.1	3.61	4.04	3.73	5.09	3.5	2.9	2.13	2.23	3.552
Carbon	5.08	5.26	5.68	7.29	5.88	5.76	4.34	4.52	5.61	3.05	5.247

5. Inorganic fiber results

At normal incidence Carbon had a higher cut resistance that S-glass. Generally, as the longitudinal angle of incidence increased, the cut resistance of the S-glass increased while the carbon fiber decreased only slightly. As the transverse angle of incidence increased, the cut resistance of the inorganic fibers decreased. S-glass has higher cut resistance than carbon fiber at 0-45. Carbon has higher cut resistances than s-glass at 0-0 and 45-0. Carbon had higher standard deviation and more random response to cut resistance testing. Being that no microscopic techniques were used, it was unclear as if single fibers of carbon were being tested as opposed to multiple fibers.

6. Microscopy of failed fibers

Scanning electron microscopy was done with a Hitachi S-4700 (Chiyoda, Tokyo, Japan) field emission scanning electron microscope. The accelerating voltage used for the scanning electron micrographs (SEMs) was 20 KV. The working distance between the detector and the fiber was between 12 and 20 mm. The fibers, after cut testing, were sputtered with a few nanometers of platinum by a Hummer XP (Alexandria, VA) sputter machine.

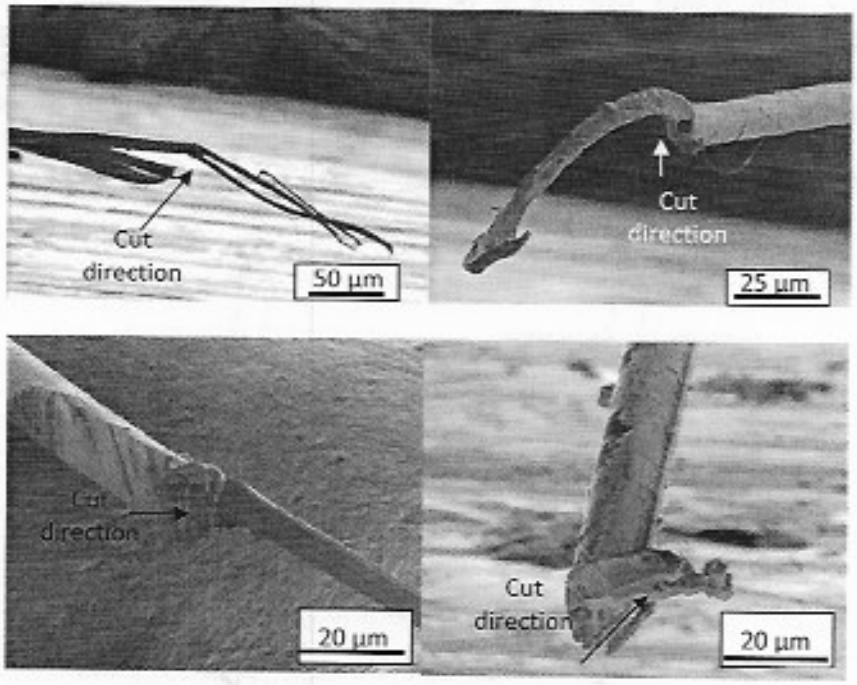
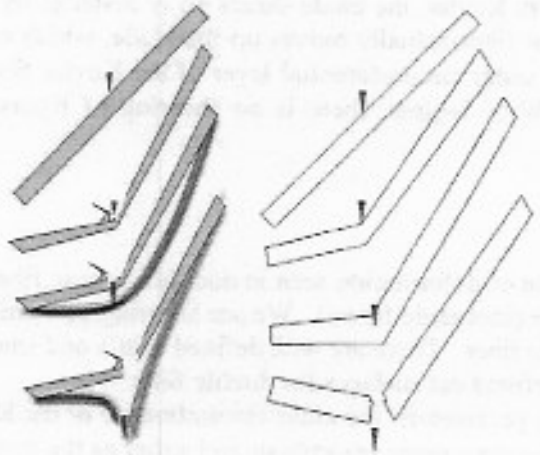


Figure 9. SEMs of (top) Kevlar after 45° longitudinal incidence cut resistance testing (0-45) and (bottom) Kevlar after cut resistance testing at 45° transverse incidence (45-0).



(a) (b)

Figure 10. Schematic of failure dynamics and cut response of (a) Kevlar and (b) S-glass fibers after 45° longitudinal cut testing (0-45).

Figures 9 shows the SEMs of the damaged areas of the tested fibers and Fig. 10 shows the damage progression of the Kevlar and S-glass fibers at 45° longitudinal cut resistance testing. The blade shears away a layer of the Kevlar shell as it moves down the 45° fiber. The blade then

resistance. With S-glass, the pattern rises instead of decreases. As the angle increases for S-glass, the blade has to go through more material. In turn, this creates a higher cut resistance.

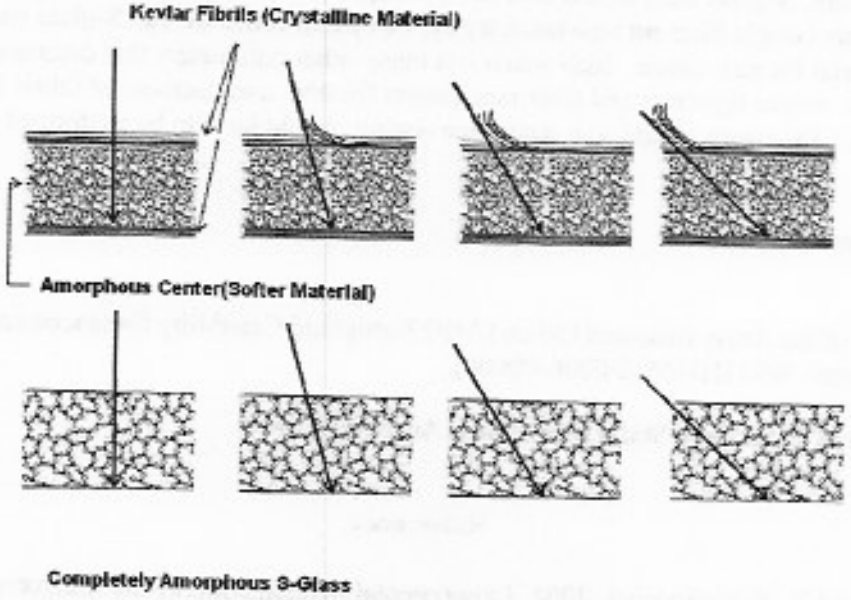


Figure 12. Model used to explain cut resistance of organic and inorganic fibers.

Fiber structure and fiber hardness are the material properties predict cut resistance

V. Conclusions

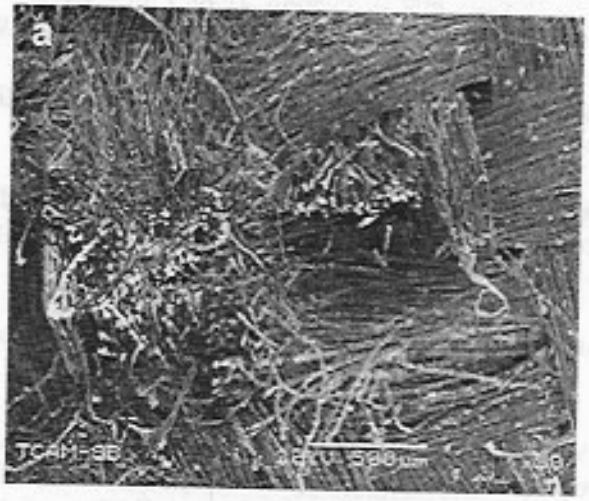


Figure XX. Kevlar fabric that has been tested for S2 knife resistance.

Educational Training Center), Susono City, Shizuoka, Fibrous Materials Research Group, Kyoto University and The Textile Machinery Society of Japan.

Liu, Q., D. Tasis, M. Prato, and H. D. Wagner. 2007. Tensile Mechanics of Electrospun Multiwalled Nanotube/Poly(methyl methacrylate) Nanofibers. *Advanced Materials* v19 pgs. 1228-1233

Mayo, J., Eric D. Wetzel, Mahesh V. Hosur and Shaik Jeelani 2009. Stab and Puncture Characterization of Thermoplastic Impregnated Aramid Fabrics. International Journal of Impact Engineering.

Nascimento, E. M. and C. M. Lepeinski. 2006. Mechanical Properties of Optical Glass Fibers Damaged by Nanoindentation after Water Aging. Journal of Non-Crystalline Solids. 352 no. 32-35: 3556-3560.

Rhorer, R., J. Chin, A. Forster, W. Chen, B. Song, X. Nie. Aging Effects on the Dynamic Tensile Response of Fibers. An Official Contribution of the National Institute of Standards and Technology.

Shin, H. S., D. C. Erlich, and D. A. Shockey. 2003. Test for measuring cut resistance of yarns. *Journal of Materials Science* 38: 3603-3610.

Shin, H. S., D. C. Erlich, Simons, J. W., and D. A. Shockey. 2006. Cut Resistance of High Strength Yarns. *Textile Research Journal* 76 no. 8: 607-613.

Singletary, J., H. Davis, M. K. Ramasubramanian, W. Knoff, and M. Toney. 2000. The transverse compression of PPTA fibers: Part I: Single fiber transverse compression testing. *Journal of Materials Science*. 35 pgs. 573-581.

Walker, A., C. Nicol, and E. K. J. Chadwick. 2004. Evaluation of test regimes for stab-resistant body armor. *Proc. Instn. Mech. Engrs., Part L (Journal of Materials:Design and Applications)* 218 no. L4: 355-361.

flexibility. They have also prepared the STF from solvent exchange method. In this method colloidal silica was heated to evaporate water from colloidal solution and the evaporated amount of water was replaced with an equivalent amount of ethylene glycol. This process continued until all the water was replaced with 57% or 62% of ethylene glycol by volume. The rheological measurements of these samples also showed a shear thickening behavior [24,25].

Recently high-power ultrasound irradiation has been extensively used in the dispersion of nanoparticles in liquids [26,27] and it is also considered as one of the efficient techniques to disperse nanoparticles into materials [28,29]. Intense ultrasound waves traveling in liquids generate growing cavities. When the cavity attains a critical size it implodes, generating extreme conditions of intense heat and tremendous pressure that provide an unusual chemical environment for chemical reactions. The formation, growth, and implosive collapse of bubbles in a liquid irradiated with ultrasound are the physical phenomenon responsible for most of the sonochemistry. Ultrasound is produced in liquids by means of piezoelectric or magnetostrictive materials: materials that expand or contract when they are placed in electromagnetic fields. Exposing such materials to a field alternating at an ultrasonic frequency produces ultrasound [30–34].

In the present investigation, we have used a high intensity ultrasonic irradiation technique for synthesis of STF. PEG is used as suspending liquid phase because of its non-toxicity, thermal stability, easy to handle and easily available in bulk quantities which make it useful for bulk production. In this technique we have also used ethanol as a solvent because its sonochemical effects have been well studied [35,36] and also it is used as a solvent in the impregnation process of STF on Kevlar and nylon fabric for body armor applications.

2. Experimental work

2.1. Materials

Colloidal silica and dry powder silica nanoparticles have been used for this study. The dry powder silica nanoparticles are spherical in shape and ~15 nm in size. These nanoparticles were purchased from Nanostructured and Amorphous Materials, Inc., Los Alamos, NM. The 200 nm spherical colloidal silica solution (MP-1040 40% concentration of silica nanoparticles) was purchased from Nissan Chemicals, Japan. PEG-200 and ethyl alcohol were purchased from Sigma–Aldrich Chemicals, St. Louis, MO.

2.2. Synthesis of shear thickening fluid

Different STF samples were prepared using different weight fraction of silica nanoparticles in PEG/ethanol by sonochemical technique. Known weight percentages of PEG and silica nanoparticles (dry powder or colloidal silica solution) were mixed in an excess amount of ethanol (40:60 STF:ethanol ratio was used) (one and half times more than STF) for colloidal silica solution no ethanol was used. The reaction mixture was irradiated with high intensity ultrasonic horn (Ti-horn, 20 kHz, 100 W/cm^2 at 50% amplitude) for 5 h and the reaction temperature was maintained using a chiller at 10 °C. The solvent (water or ethanol) was later removed from the reaction mixture via an evaporation process by heating at about 100 °C. The concentrations of as-prepared STF samples (sample (A)–sample(I)) are presented in Table 1.

For comparison purposes STF sample (I) was synthesized using mechanical mixing method.

In this method a known weight percentage of silica powder and PEG were mixed for 10 min at room temperature using a THINKY hybrid mixer ARE-250.

2.3. Characterization

2.3.1. Rheological measurements

Rheological studies were performed for all as-prepared STF samples to investigate the effect of shear rate increase on the viscosity. These tests were carried out using a TA Instrument Rheometer-AR2000 at room temperature, 0 °C and 40 °C. All the test were carried out using a peltier plate and a cone plate of size 40 mm and 2° angles in a steady state flow mode and shear ramp rate of 0–125 s^{-1}.

2.3.2. Thermal analysis

Thermogravimetric analyses (TGA) experiments were conducted to estimate the weight ratios of silica and polyethylene glycol in as-prepared STF samples. TGA samples were prepared by adding a few drops of as-prepared STF samples (10–20 mg) to a known weight of alumina crucible. TGA experiments were carried out using a Mettler Toledo TGA/SDTA 851 from room temperature to 800 °C at heating rate of 5 °C/min under nitrogen atmosphere.

2.3.3. Scanning electron microscopy (SEM)

SEM studies were carried out using a JEOL JSM 5800 scanning electron microscope. The SEM samples were prepared by uniformly spreading the as-prepared STF samples on a double-sided carbon tape and coated with gold/palladium to prevent charge buildup by the electron absorption.

2.3.4. Transmission electron microscopy (TEM)

TEM investigation of as-received silica nanopowder and colloidal silica nanoparticles were carried out using a JOEL-2010 microscope. TEM samples were prepared by dispersion of nanoparticles in ethanol and a drop of solution was placed on a copper grid (carbon coated copper grid-200 mesh) then dried in air and used for TEM analysis.

3. Results and discussion

The rheological properties of as-prepared STF samples were studied to understand shear thickening or shear thinning behavior rate at room temperature. Fig. 1A shows the viscosity of STF sample (A) as a function of the shear rate. STF sample (A) demonstrates shear thickening behavior in the range of 10–30/s shear rate and the sample viscosity increases from ~2 Pa s to ~17 Pa s. Fig. 1B (sample B), with a lower concentration of silica nanoparticles (52 wt%), shows a shear thickening effect in the range of ~2–40/s shear rate and with increase in the viscosity from 2.5 Pa s to 8 Pa s before a reversible trend is seen. The rheological properties of STF samples (sample (A) and sample(B)) indicate that the increase of the weight fraction of the suspending phase (PEG) in the sample gives better shear thickening fluid as the samples become more viscous. Fig. 2C shows the rheological graph of sample (C) where the silica weight fraction was decreased to 42 wt % and the weight fraction of PEG was increased to 58 wt%. This Fig. 2C shows a significant shear thickening behavior with an increase in the viscosity from ~10 Pa s to ~270 Pa s between 7 and 20/s shear rates. The increased value of viscosity indicates that the sample exhibits an incredibly high shear thickening effect. Sample (D) contains a relatively larger amount of PEG (60 wt%) and shows a shear thickening behavior. These results are presented in Fig. 2D and the viscosity changes from ~20 Pa s at 5/s shear rate to 410 Pa s at 12/s shear rate before a reversal trend is seen. Shear rate values for shear thickening transitions are lower than the results reported in similar studies [23]. These results clearly show that the sonochemical mixing before evaporation significantly improves the shear thickening effect. The rheological graph of STF sample (E)

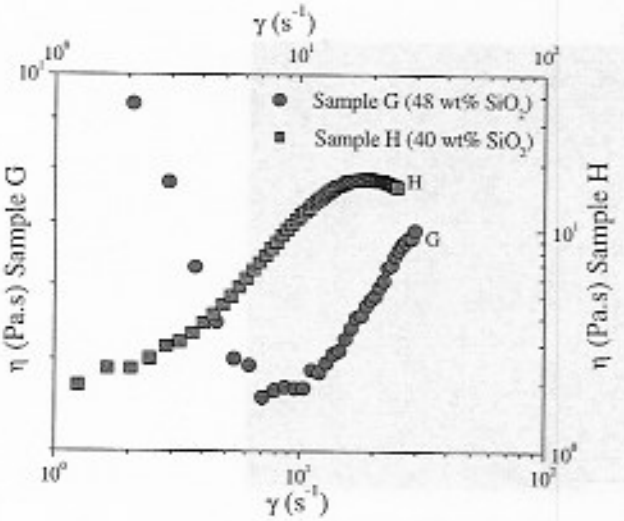


Fig. 4. Rheology graph of STF Sample G and STF Sample H.

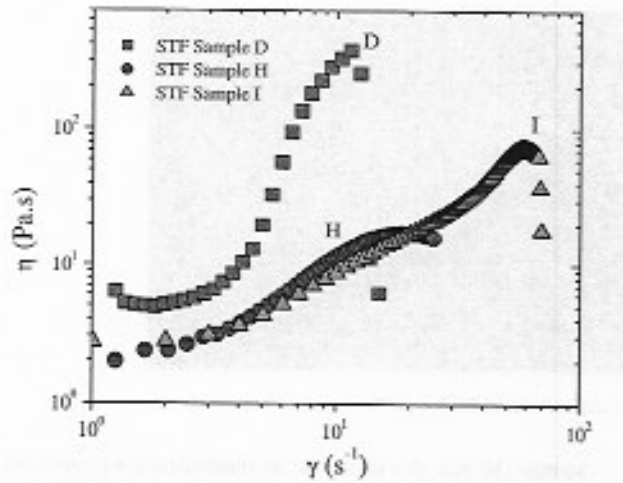


Fig. 5. Rheology graph of STF Samples D, H and I.

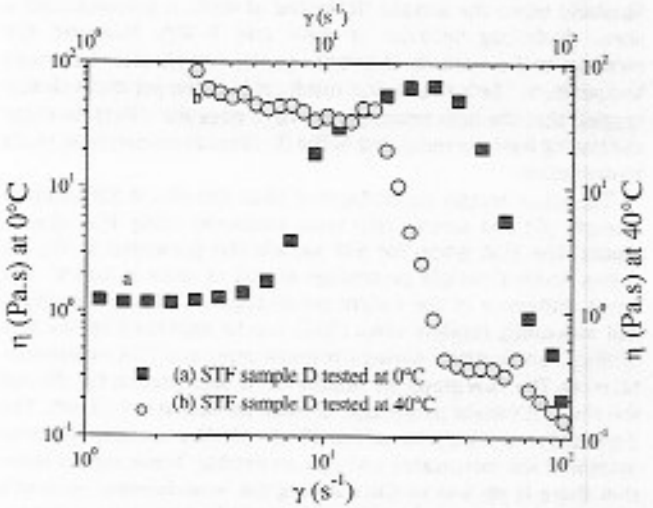


Fig. 6. Rheology graph of STF sample D tested at (a) 0 °C and (b) 40 °C.

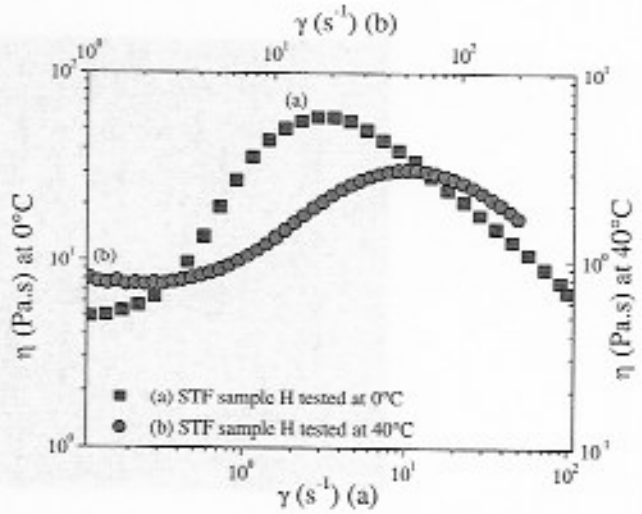
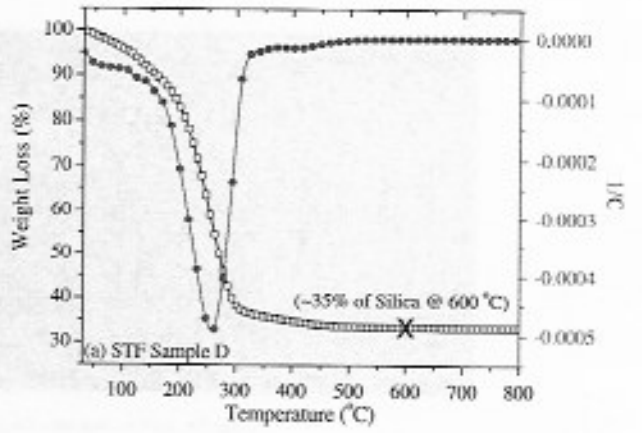


Fig. 7. Rheology graph of STF sample H tested at (a) 0 °C and (b) 40 °C.



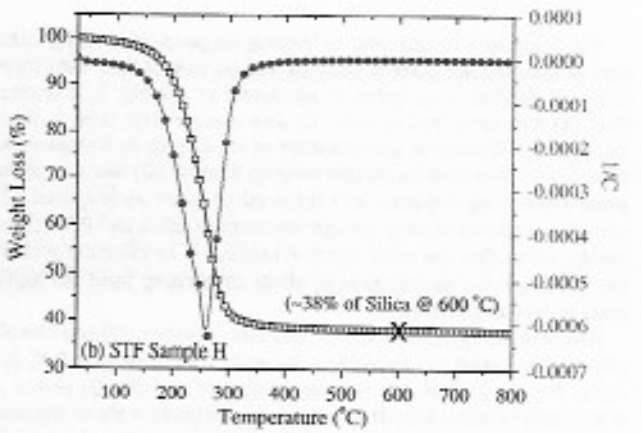


Fig. 8. TGA graphs for (a) STF sample D and (b) STF Sample H.

STF sample (I) was prepared using the same weight fractions (40 wt% of dry silica nanoparticles and 60 wt% of PEG) as in case of sample (D) and sample (H) for comparison purpose. The sample (I) is prepared using a simple mixing for 10 min instead of ultrasonic irradiation. The as-prepared homogeneous fluid was characterized for its rheological properties and shown in Fig. 5I. These results show a shear thickening behavior at shear rate range of 2–79/s with an increase in the viscosity from ~1 Pa s to ~57 Pa s.

solvents and they are pure STF. These TGA results also suggest that the smaller powder (15 nm) nanoparticles show more errors in weight fraction calculations as compared to the larger (200 nm) colloidal particles.

TEM micrographs of as-received silica nanoparticles and colloidal silica solution are shown in Fig. 9a and b, respectively. The as-received silica nanoparticles are spherical in shape and the particles sizes measured from Fig. 9a are ~5–15 nm agglomerates. Fig. 9b shows the TEM image of as-received colloidal silica solution and the particles are highly spherical in shape and mono dispersed. No agglomerates were observed and the particles size measured ~200 nm.

To further study the dispersion of silica nanoparticles in PEG, the SEM analyses were carried out on as-prepared STF samples. Fig. 10 shows the SEM micrographs of STF samples (sample (D) and sample (H)). Fig. 10 shows that the silica nanoparticles are well coated with PEG. Fig. 10a shows larger particle agglomerations as compared to Fig. 10b which is expected because of the large particles size differences in the starting materials and smaller nanoparticles are know to agglomerates more than the larger particles. These results are consistence with observed shear thickening behavior.

4. Conclusion

Efficient and one-pot sonochemical method has been developed to synthesize shear thickening silica dispersions. Unlike previous reports, here we have synthesized the shear thickening fluid using a dry silica nanopowder or colloidal silica solution. The main advantage of this synthesis technique compared to previous methods is that our method produces a better shear thickening transition at lower shear rate and drastically reduced the water content contamination. This sonochemical synthesis technique can also be used to synthesize larger quantities of STF samples for verity of applications including liquid body armor. The high temperature results suggest that these STFs loose its shear thickening behavior at high temperatures and more studies needs to be carried out to understand the temperature effect.

Acknowledgements

This work is supported by the United States Army Research Office (ARO). The authors would like to thank Dr. Norman Wagner, Department of Chemical Engineering, University of Delaware, and Dr. Eric Wetzel, Army Research Laboratory (ARL) for their valuable suggestions.

References

[1] H.A. Barnes, J. Rheol. 33 (1989) 329.
[2] J. Freundlich, J. Juliusberger, Trans. Faraday Soc. 31 (1935) 920.
[3] R.L. Hoffmann, Tran. Soc. Rheol. 16 (1972) 155.
[4] R.L. Hoffmann, J. Colloid Interf. Sci. 46 (1974) 491.
[5] R.L. Hoffmann, Sci. Technol. Polym. Colloids 2 (1983) 570.
[6] W. Boersma, J. Laven, H.N. Stein, J. Colloid Interf. Sci. 149 (1992) 10.
[7] H. Laun, H.M. Laun, R. Bung, S. Hess, W. Loose, O. Hess, K. Hahn, E. Hadicke, R. Hingmann, J. Rheol. 36 (1992) 743.
[8] L.M. Zhang, J.F. Zhou, P.S. Hui, Colloid Surf. Physicochem. Eng. Aspects 259 (2005) 189.
[9] J.W. Bender, N.J. Wagner, J. Rheol. 40 (1996) 899.
[10] T.N. Phung, J.F. Brady, G. Bossis, J. Fluid Mech. 313 (1996) 181.
[11] J. Melrose, J. van Vliet, R. Ball, Phys. Rev. Lett. 77 (1996) 4660.
[12] R.S. Farr, J.R. Melrose, R.C. Ball, Phys. Rev. 55 (1997) 7203.
[13] J.F. Brady, G. Bossis, Annu. Rev. Fluid Mech. 20 (1988) 111–157.
[14] J.W. Bender, N. Wagner, J. Colloid Inter. Sci. 172 (1995) 171.
[15] B.J. Maranzano, N. Wagner, J. Chem. Phys. 117 (2002) 10291.
[16] G. Bossis, J.F. Brady, J. Chem. Phys. 91 (1989) 1866.
[17] C.G. Albert, TAPPI 34 (1951) 453.
[18] B. Alince, P. Lepoutre, TAPPI 06 (1983) 57.
[19] S.D. Choi, Ph.D. thesis, Ann Arbor, MI, 1983.
[20] E.J.W. Verwey, J.H. de Boer, Rec. Trav. Chim. 57 (1939) 383.
[21] Z. Andreja, L. Romano, Z. Miha, TAPPI 30 (1997) 67.
[22] S.R. Raghavan, S. Khan, J. Colloid Inter. Sci. 185 (1997) 57.
[23] S. Lee, E. Wetzel, N. Wagner, J. Mater. Sci. 38 (2003) 2825.
[24] R. Egres Jr., M. Decker, C. Halbach, S. Lee, J. Kirkwood, K. Kirkwood, N. Wagner, Army Sci. Conf. (2004).
[25] S. Lee, E. Wetzel, R. Egres Jr., N. Wagner, Army Sci. Conf. (2002).
[26] C. Sauter, M.A. Emin, H.P. Schuchmann, S. Tavman, Ultrason. Sonochem. 15 (2008) 517.
[27] M. Toan, N. Tsing, T. Tsung, H. Chang, J. Vac. Sci. Technol., B 27 (2009) 1586.
[28] M.H. Choi, I.J. Chung, D.J. Lee, Chem. Mater. 12 (2000) 2977.
[29] I.G. Eskin, Ultrason. Sonochem. 8 (2001) 319.
[30] K. Suslick, Sci. Am. (1989).
[31] K. Suslick, Modern Synth. Methods 4 (1986) 1.
[32] P. Boudjouk, J. Chem. Educ. 63 (1986) 427.
[33] K. Suslick, B. Edward, Flint Nature 330 (1987) 553.
[34] K. Suslick, VCH Publishers, Inc., 1988.
[35] L.A. Pérez-Maqueda, A. Duran, J.L. Pérez-Rodríguez, Appl. Clay Sci. 28 (2005) 245.
[36] F. Franco, J.A. Cecila, L.A. Pérez-Maqueda, J.L. Pérez-Rodríguez, C.S. Gomes, Appl. Clay Sci. 35 (2007) 119.
[37] S.X. Ma, S.L. Cooper, Macromolecules 34 (2001) 3294.
[38] G.N. Choi, I.M. Krieger, J. Colloid Interf. Sci. 113 (1986) 101.

B) Introduction of Styrene:

Styrene is the simplest molecule that contains an unsaturated group covalently linked to an aromatic ring and therefore represents a model candidate to be added with Silane-Gluta armor system for enhanced bonding. Since initially Spectra provided better knife performance, various weight percentage of styrene was added to the silane-Gluta system. After several trials, 50 wt% of styrene was found to be the optimum concentration. That is - styrene was 50wt% of the total polymer (silane + Gluta + Styrene). Any higher concentration above 50 wt% did not improve knife performance. Results from NIJ knife tests are shown in Fig. 2. It is observed that energy for zero layer penetration has increased from 6 J-cm^2/g to 14 J-cm^2/g – about 133% improvement. Energy levels for 1-4 layer penetrations were also higher as seen in Fig. 2 suggesting styrene to be an effective reinforcement for better knife performance.

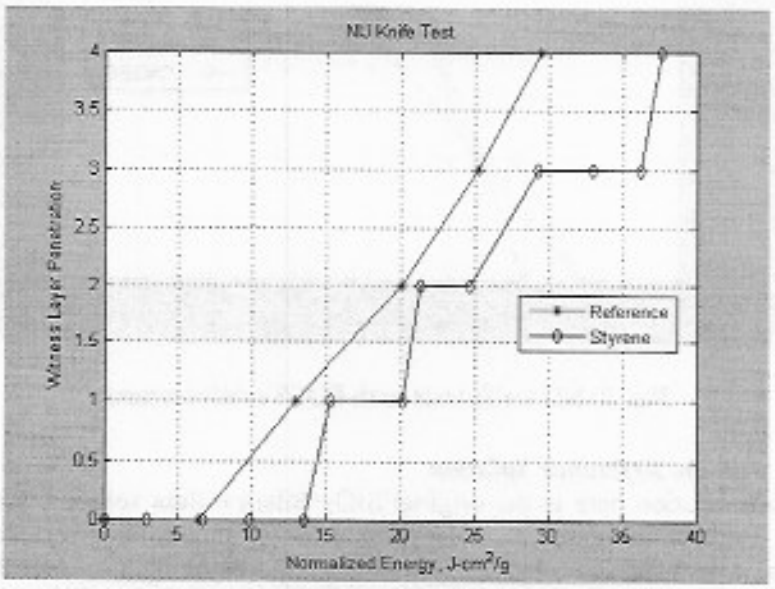


Fig. 2: NIJ Knife tests with styrene reinforcement

C) Use of POSS (polyhedral oligomeric silsesquioxane)

POSS is a nanostructured organic-inorganic hybrid polymer with a cubic structure having eight silicon atoms at the core and linked to 12 oxygen atoms. The advantage of using POSS is that these silicon atoms can be linked to a substituent that can be almost any chemical group known in organic chemistry. Chemically bonded POSS with thermoset or thermoplastic polymers either enhances or reinforces the mechanical and thermal properties of the neat material system. POSS is available commercially (Hybrid Plastics) with a multitude of functional groups. Since POSS is more like a silica molecule (1-2 nm in size) than a nanoparticle, our intention was to replace SiO_2 nanoparticles that we have used so far. Three types of POSS were used in the investigation. The types were identified according to their functional groups; trisilanol, CAO299X, and CAO300X. The last two categories were carboxylic acid based and had an aromatic ring structure attached to their reactive group. The procedure to use POSS was identical to that of SiO_2 since all three categories of POSS were soluble in ethanol. Results from NIJ knife tests are shown in Fig. 3. It is observed that knife resistance with CAO300X system is around 10 J-cm^2/g for zero layer penetration. However this value is lower than 14 J-cm^2/g observed earlier with styrene. It is to be noted that we were able to procure only a small

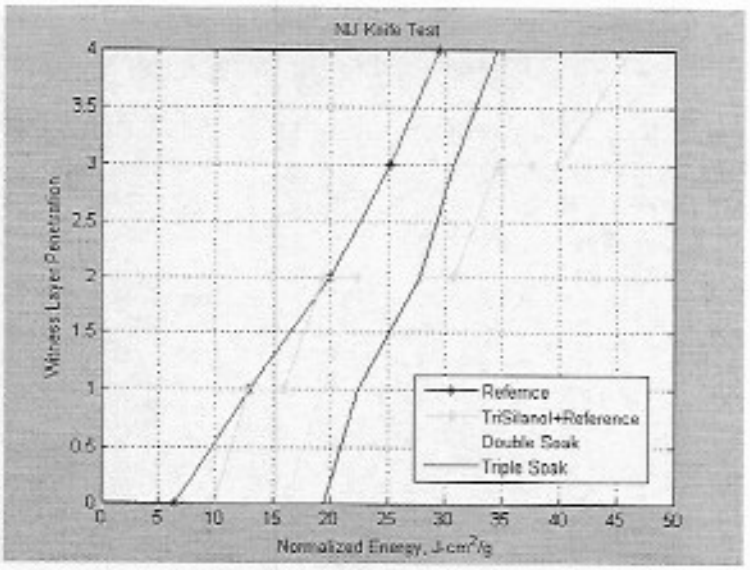


Fig. 4: NIJ Knife tests with multiple soaks

Micro-Droplet Tests:

It was clear from the current knife tests as well from spike tests conducted during previous years that a good amount of impact energy was absorbed by friction between fiber and the surrounding particle-polymer mixture. This friction arises as the fibers tend to dynamically slide during impact. Micro-droplet tests were conducted to assess the interface shear stress and associated energies. The most challenging task was to prepare specimens for micro-droplet tests since the matrix viscosity changed with the addition of silica and Gluta.

A set up was made with flat plate with two raised ends (parallel to each other) and the fibers were held tight for droplet application. A droplet applicator was made by using a regular toothpick with a fiber taped onto it. The applicator was dragged through the particle-polymer mixture, and applied to the fiber in one steady stroke. Droplets were then cured in an oven in horizontal position. The viscosity of silane-silica-Gluta mixture was carefully controlled by drying the mixture after sonication. Drying time varied depending on the amount of ethanol present in the solution. Droplets were around 150-200 μm in size as shown in Fig. 5. After curing, the droplets were cut off the plate with a fiber length of about 12.5 mm having droplet in the middle. They were then glued to a capillary tube at one end and a hook glued to the other end of the tube to hang the sample. Measurements were then taken for the following: droplet length (l), fiber diameter (d), and the length from the capillary tube to the tip of the droplet. Measurements were taken through a microscope.

Micro-droplet specimens were taken to University of Delaware and tests were performed there. The test set up consisted of a load cell, two light sources, two cameras (one horizontal and one vertical) with video monitors, two parallel blades, and a motor controller to move the specimen up and down. The test set up is shown in Fig. 6. The distance between the blades is moved manually, but viewed by the vertical camera. The motorized movement and application of load were controlled by a custom LabView program. A sample load displacement curve obtained from the tests is shown in Fig. 7.

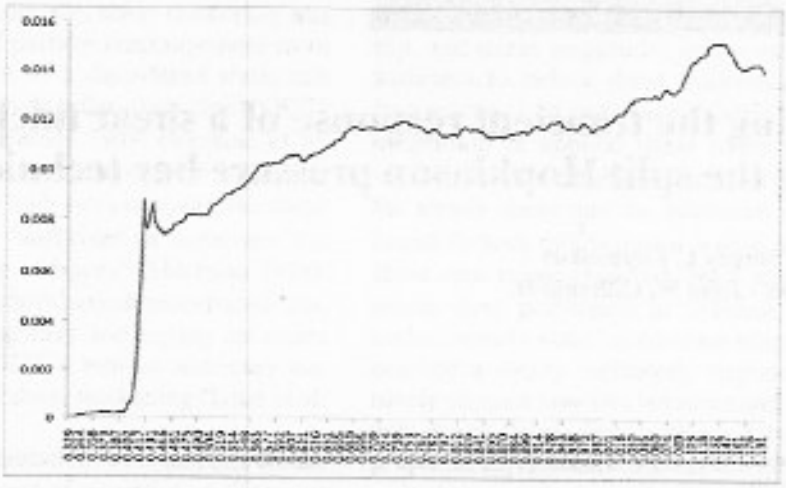


Fig. 7: Load vs. displacement curve from micro droplet test

Summary:

It has been shown that knife resistance of Kevlar is extremely weak compared to that of Spectra. Energy absorption by Spectra with regular solution of silane+silica+Gluta is still low but can be substantially increased by addition of styrene and POSS to the solution. Especially, multiple soaking up to three times was very effective – it enhanced knife resistance from 6 J-cm^2/g to 20 J-cm^2/g. Micro droplet tests were performed in collaboration with University of Delaware and it was demonstrated that friction at the fiber/matrix interface was responsible for absorption of most of the energy during spike or knife penetration.